

Numerical Investigation of Effective Moduli of Porous Elastic Material with Surface Stresses for Various Structures of Porous Cells



A. V. Nasedkin and A. S. Kornievsky

Abstract The chapter deals with the model problem of finding the effective moduli of a nanoporous elastic material, in which the surface stresses are defined on the pore surface to reflect the size effect using the Gurtin–Murdoch model. One cell of a porous material in the form of a cube with one pore located in the center is considered. The objective of the study is to assess the influence of the pore shape and the magnitude of the scale factors on the effective moduli of the composite material. The homogenization problem is formulated within the framework of the effective moduli method, and to find its solution, the finite element method and the ANSYS software package are used. In the finite element model, the surface stresses are taken into account by membrane elements covering the pore surfaces and conformable with the finite element mesh of bulk elements. Numerical experiments carried out for pores of cubic and spherical shapes show the cumulative significant effect of pore geometry and scale factors on the effective elastic moduli.

1 Introduction

The problems of nanomechanics remain extremely relevant for the last few years. Numerous studies have revealed a scale effect, which consists in changing the effective stiffness and other material moduli for nanoscale bodies in comparison with the corresponding values for bodies of usual macro-dimensions. A number of theories have been developed to explain the scale factor. One of these widely used theories is the model of surface elasticity. There are a number of reviews [10, 16, 35, 36] devoted to research on the surface theory of elasticity and its applications. In turn, among the theories of surface elasticity, the most popular is the Gurtin–Murdoch

A. V. Nasedkin (✉) · A. S. Kornievsky
Institute of Mathematics, Mechanics and Computer Science, Southern Federal University,
Milchakova Street 8a, Rostov-on-Don 344090, Russia
e-mail: nasedkin@math.sfedu.ru

A. S. Kornievsky
e-mail: alexandr5koren@gmail.com

© Springer Nature Switzerland AG 2019
M. A. Sumbatyan (ed.), *Wave Dynamics, Mechanics and Physics of Microstructured Metamaterials*, Advanced Structured Materials 109,
https://doi.org/10.1007/978-3-030-17470-5_15

model [15]. The use of this model actually leads to the fact that the boundaries of the nano-sized body are covered with elastic membranes, the internal forces in which are determined by surface stresses. Elastic membranes can be placed at the interphase boundaries inside the body with nanoscale inclusions, which makes it possible to simulate imperfect interface boundaries with stress jumps [3–5, 7, 8, 14, 24].

The Gurtin–Murdoch model was repeatedly used to describe elastic nanostructured composites. Thus, in [1, 2, 6–9, 11, 22, 23, 31] and others, within the framework of the theory of elasticity with surface stresses, the mechanical properties of composites with spherical nano-inclusions (nanopores), as well as fibrous and other nanocomposites, were investigated. Techniques of finite element approximation for elastic materials with surface effects and examples of calculations are presented in [12, 13, 17–21, 26–28, 32, 34] and others.

In this paper, we study the effective stiffness properties of a nanoporous isotropic elastic material for various forms of pores. Porous material is considered as a limiting case of a two-phase mixed composite, when the material of inclusions has negligibly small stiffness moduli. The nano-dimensionality at the boundaries of the material with pores was taken into account using the Gurtin–Murdoch surface stress model. This paper is a continuation of research [26–30]. In the development of the above-mentioned paper, the scale factor is associated with the pore size and the effect of pore shape on the effective composite properties is studied.

2 Mathematical Problem Statement

Let Ω be a unit cubic cell of elastic porous material with one pore of cubic or spherical form; a is the cubic cell side; $\Omega = \Omega^{(1)} \cup \Omega^{(2)}$; $\Omega^{(1)}$ is the part of Ω with main elastic material; $\Omega^{(2)}$ is the pore; $\Gamma = \partial\Omega$ is the external boundary of the cell; $\Gamma^s = \partial\Omega^{(2)}$ is the boundary of the pore; n_k are the components of the unit normal vector external with respect to the volume of the main elastic material $\Omega^{(1)}$.

The unit cell Ω is linked to the Cartesian coordinate system $Ox_1x_2x_3$ so that it occupies the region $|x_k| \leq a/2$. Then, in the case of a cubic pore with side b ($b < a$), the domain $\Omega^{(2)}$ will be defined by the inequalities $|x_k| \leq b/2$, and in the case of a spherical pore with radius R , the domain $\Omega^{(2)}$ is given by the inequality $r \leq R$, $r = \sqrt{x_1^2 + x_2^2 + x_3^2}$.

We will assume that in the volume Ω the system of equations of the static theory of elasticity is satisfied with respect to the components $u_k = u_k(\mathbf{x})$ of the displacement vector

$$\partial\sigma_{ij}/\partial x_j = 0, \quad \sigma_{ij} = \lambda\varepsilon_{kk}\delta_{ij} + 2\mu\varepsilon_{ij}, \quad \varepsilon_{ij} = (\partial u_i/\partial x_j + \partial u_j/\partial x_i)/2, \quad (1)$$

where σ_{ij} and ε_{ij} are the components of the stress and strain tensors, respectively; λ , μ are the Lamé's coefficients; δ_{ij} is the Kronecker symbol.

Here we consider the pore as an elastic material with negligible Lamé's coefficients. Thus, the system of equations (1) is satisfied in Ω , with $\lambda = \lambda^{(m)}$, $\mu = \mu^{(m)}$ for $\mathbf{x} \in \Omega^{(m)}$; $\lambda^{(2)} \ll \lambda^{(1)}$, $\mu^{(2)} \ll \mu^{(1)}$.

We will accept that the pore $\Omega^{(2)}$ is nanosized and in accordance with the Gurtin–Murdoch model, at its boundary Γ^s the surface stresses σ_{ij}^s exist, and the following equations hold

$$n_j[\sigma_{ij}] = \partial^s \sigma_{ij}^s / \partial x_j, \quad \mathbf{x} \in \Gamma^s, \tag{2}$$

$$\sigma_{ij}^s = \lambda^s \varepsilon_{kk}^s \delta_{ij} + 2\mu^s \varepsilon_{ij}^s, \quad \varepsilon_{ij}^s = (\partial^s u_i^s / \partial x_j + \partial^s u_j^s / \partial x_i) / 2, \tag{3}$$

$$\partial^s / \partial x_j = \partial / \partial x_j - n_j(n_k \partial / \partial x_k), \quad u_i^s = (\delta_{ik} - n_i n_k) u_k, \tag{4}$$

where $[\sigma_{ij}] = \sigma_{ij}^{(1)} - \sigma_{ij}^{(2)}$ is the stress jump over the boundary Γ^s between the volumes with different materials; $\partial^s / \partial x_j$ are the components of the surface nabla-operator; λ^s, μ^s are the surface Lamé's coefficients; ε_{ij}^s are the surface strains; u_i^s are the surface displacements.

In the rectangular local coordinate system, attached with tangent ords $\tilde{\mathbf{e}}_1 = \boldsymbol{\tau}_1$, $\tilde{\mathbf{e}}_2 = \boldsymbol{\tau}_2$ and normal $\tilde{\mathbf{e}}_3 = \mathbf{n}$, the sets of the values $\tilde{u}_i^s, \tilde{\varepsilon}_{ij}^s, \tilde{\sigma}_{ij}^s$ are pertaining to surface, i.e. $\tilde{u}_3^s = 0, \tilde{\varepsilon}_{13}^s = \tilde{\varepsilon}_{23}^s = \tilde{\varepsilon}_{33}^s = 0, \tilde{\sigma}_{13}^s = \tilde{\sigma}_{23}^s = \tilde{\sigma}_{33}^s = 0$.

Note that as we can see from Eq. (1) the surface stresses σ_{ij}^s have the dimensionality (N/m) different from the dimensionality (N/m²) of usual bulk stresses σ_{ij} . Also the surface Lamé's coefficients λ^s, μ^s have the dimensionality (N/m) different from the dimensionality (N/m²) of usual bulk Lamé's coefficients λ, μ .

When calculating the effective moduli of a porous elastic material with surface stresses, we will find the basic moduli that are important for practical applications. As is well known, for elastic isotropic materials such moduli are the stiffness moduli c_{11}, c_{12} , the Young's modulus E , the Poisson's ratio ν , the shear modulus $G = \mu = c_{44}$, and the bulk modulus K . These moduli can be expressed through the Lamé's coefficients by the following formulae

$$c_{11} = \lambda + 2\mu, \quad c_{12} = \lambda, \quad E = \frac{\mu(3\lambda + 2\mu)}{\lambda + \mu}, \quad \nu = \frac{\lambda}{2(\lambda + \mu)}, \quad K = \lambda + \frac{2}{3}\mu, \tag{5}$$

or through the Young's modulus and the Poisson's ratio

$$\lambda = \frac{\nu E}{(1 + \nu)(1 - 2\nu)}, \quad \mu = \frac{E}{2(1 + \nu)}, \quad K = \frac{E}{3(1 - 2\nu)}. \tag{6}$$

Similarly, instead of the surface Lamé's coefficients λ^s and μ^s we can use other surface moduli. For example, we can introduce the surface Young's modulus E^s and the surface Poisson's ratio ν^s having expressed from the first formula (3) the surface strains ε_{ij}^s through the surface stresses σ_{ij}^s in a form similar to the standard Hooks's law for the three-dimensional theory of elasticity

$$\varepsilon_{ij}^s = -\frac{\nu^s}{E^s} \sigma_{kk}^s \delta_{ij} + \frac{(1 + \nu^s)}{E^s} \sigma_{ij}^s. \quad (7)$$

Since in (3) and in (7) the surface quantities are related, the expressions for the surface moduli will differ from (5), (6) [19]

$$c_{11}^s = \lambda^s + 2\mu^s, \quad c_{12}^s = \lambda^s, \quad E^s = \frac{4\mu^s(\lambda^s + \mu^s)}{\lambda^s + 2\mu^s}, \quad \nu^s = \frac{\lambda^s}{\lambda^s + 2\mu^s}, \quad K^s = \lambda^s + \mu^s, \quad (8)$$

$$\lambda^s = \frac{\nu^s E^s}{1 - (\nu^s)^2}, \quad \mu^s = \frac{E^s}{2(1 + \nu^s)}, \quad K^s = \frac{E^s}{2(1 - \nu^s)}. \quad (9)$$

Here, in (8), (9) we define the surface compression modulus K^s in the form corresponding to [1, 19, 24] and differ from [6–8] and others.

Thus, a nanoporous composite with surface stresses on the pore boundaries is characterized by four elastic moduli, for example, $E^{(1)}$, $\nu^{(1)}$, E^s and ν^s ($E^{(2)} \approx 0$). We will assume that the “equivalent” homogeneous material will be isotropic and will be characterizes by two independent moduli, for example, by c_{11}^{eff} and c_{12}^{eff} . In order to find these effective moduli, it is enough to solve the problem (1)–(4) in the unit cell Ω with the boundary conditions

$$u_1 = \varepsilon_0 x_1, \quad u_2 = u_3 = 0, \quad \mathbf{x} \in \Gamma, \quad (10)$$

where $\varepsilon_0 = \text{const}$.

After solving the problem (1)–(4), (10) similar to [26–29], we can calculate the effective stiffness moduli by using the formulae

$$c_{11}^{\text{eff}} = \langle \sigma_{11} \rangle / \varepsilon_0, \quad c_{12}^{\text{eff}} = \langle \sigma_{22} \rangle / \varepsilon_0, \quad (11)$$

where the angle brackets $\langle (\bullet) \rangle$ denote the averaged integral volume and interface values [3, 4, 18, 19]

$$\langle (\bullet) \rangle = \frac{1}{|\Omega|} \left(\int_{\Omega} (\bullet) d\Omega + \int_{\Gamma^s} (\bullet)^s d\Gamma \right). \quad (12)$$

We can check that the homogenized material will be isotropic, if for the solution of the problem (1)–(4), (10) we verify that $c_{12}^{\text{eff}} \approx \langle \sigma_{33} \rangle / \varepsilon_0$; $\langle \sigma_{jk} \rangle \approx 0$, $j \neq k$. For additional control we can solve the shear problem (1)–(4) with boundary conditions: $u_1 = 0$, $u_2 = \varepsilon_0 x_3 / 2$, $u_3 = \varepsilon_0 x_2 / 2$, $\mathbf{x} \in \Gamma$. From the solution of this problem we can anew calculate the shear modulus $c_{44}^{\text{eff}} = \langle \sigma_{23} \rangle / \varepsilon_0$, and this modulus should be approximately equal to $c_{44}^{\text{eff}} \approx (c_{11}^{\text{eff}} - c_{12}^{\text{eff}}) / 2$, where the stiffness moduli c_{11}^{eff} and c_{12}^{eff} are found from the solution of the problem (1)–(4), (10).

In conclusion of this section, we note that the model of the pore as an elastic material gives some error, but since $\lambda^{(2)} \approx 0$, $\mu^{(2)} \approx 0$, we should expect that the stress components in the pore region will also be small $\sigma_{ij}^{(2)} \approx 0$.

3 Finite Element Results and Discussion

The boundary problems (1)–(4), (10) were solved numerically in the ANSYS finite element package.

By virtue of the problem symmetry and for the convenience of analyzing the fields inside the volume, a quarter of the cell $\{-a \leq x_1 \leq a, 0 \leq x_2 \leq a, 0 \leq x_3 \leq a\}$ was considered with symmetry conditions on the faces $x_2 = 0, x_3 = 0$. Inside the cell, as a pore either a quarter cube $\{-b \leq x_1 \leq b, 0 \leq x_2 \leq b, 0 \leq x_3 \leq b\}$ (case 1), or a quarter ball $\{r \leq R, 0 \leq x_2, 0 \leq x_3\}$ (case 2) were set. The 10-node tetrahedral structural SOLID92 elements were used as volumetric elements. The presence of surface stresses was modelled with 8-node SHELL281 elements with the option of membrane stresses and with degenerate triangular 6-node shapes. The shell elements were covered the inner boundary of the pore and were located on the triangular faces of the corresponding bulk tetrahedral elements, which ensured the conformality of the finite element mesh consisting of bulk and shell elements.

The grid of bulk finite elements was created in ANSYS with a limit on the maximum size of elements equal to $\hat{a}/10$, where \hat{a} is the dimensionless cell size. Bulk elements inherit the material properties of the main elastic material and pore associated with a quarter of the volumes $\Omega^{(1)}$ and $\Omega^{(2)}$. Then, shell finite elements were created automatically on the elements faces located on the inner surface of the pore. Variants of the constructed finite element meshes without elements with the material properties of pores are shown in Fig. 1 for the case of cubic pores (a) and spherical pores (b). Shell elements in Fig. 1 highlighted in a darker, and porosity p is the same and equal to 40%.

We considered steel as the main material with the following elastic moduli: $E^{(1)} = 2 \cdot 10^{11}$ (N/m²), $\nu^{(1)} = 0.3$. In the pore volume, we set negligible stiffness moduli using the formulae: $E^{(2)} = \kappa E^{(1)}$, $\kappa = 10^{-10}$, $\nu^{(2)} = \nu^{(1)}$.

For surface moduli we accept the following formulae: $E^s = d^s E^{(1)}$, $\nu^s = \nu^{(1)}$, $d^s = 10^{-10}$ (m). Note that, unfortunately, so far there are very few data on surface moduli, and they are quite contradictory. Therefore, in a large number of theoretical papers, the same values of surface moduli from [25, 33] are used, which greatly differ in different crystallographic planes and some are negative. In this regard, here we use the model values of the surface moduli.

Analogously to [26, 27], we model in ANSYS the surface effects by using shall finite elements with the membrane stress option. For these elements we specify the Young's modulus E^m , the Poisson's ratio ν^m and thickness h^m . In order for the membrane element can be used as a surface element, we must accept: $E^s = h^m E^m$, $\nu^s = \nu^m$ [26, 27]. We also assume that $h^m = b$, $E^m = k^s E$, where k^s is a dimensionless coefficient. Then, $b = d^s / k^s$, and therefore the coefficient k^s is inversely proportional to the size b of cubic pore.

In the calculations, we determined the pore size as dimensionless, with the side of cubic pore \hat{b} being equal to 1. We set the dimensionless radius $\hat{R} = (3\pi/4)^{1/3}$ so that the volume of the spherical pore is equal to the volume of the cubic pore. The

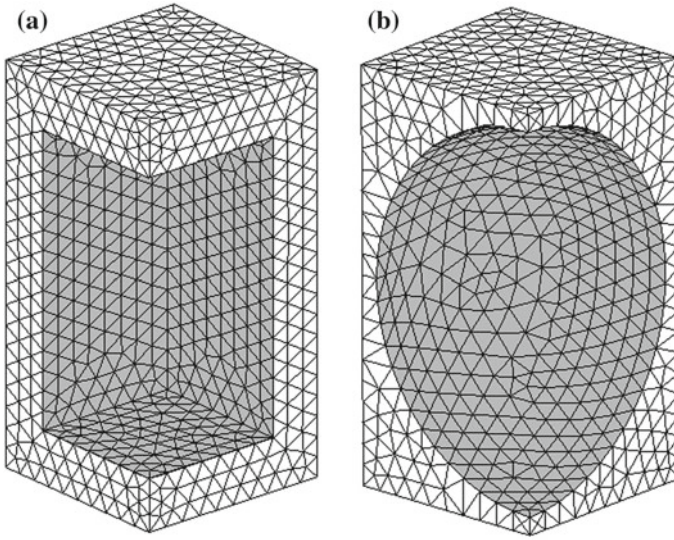


Fig. 1 Finite element mesh for two cases of quarter unit cell without pore elements

dimensionless cell size \hat{a} for both cases was determined depending on the specified percentage of porosity p : $\hat{a} = (p/100)^{-1/3} \hat{b} = (p/100)^{-1/3}$.

We analysed the influence of the pore forms, the percentage of porosity and the surface stresses on the effective moduli. We varied the percentage of porosity p from 0 to 50%, the multiplier value for surface stresses k^s , and the pore form (cube or sphere).

The results of the calculations are presented in Figs. 2, 3, 4, 5, 6 and 7. Here $r(\dots)$ designates the relative value of the effective modulus, with respect to the value of the corresponding modulus for main elastic material without pore. Thus, $r(c_{11}) = c_{11}^{\text{eff}}/c_{11}^{(1)}$, where c_{11}^{eff} is the effective stiffness modulus for the porous material with or without interface stresses, $c_{11}^{(1)}$ is the value of the corresponding stiffness modulus for the dense main material, and so on. The curves 1 correspond to the case of porous material without surface stresses, when $k^s = 0$; the curves 2 correspond to the case of porous material with small surface stresses, when $k^s = 0.1$; the curves 3 correspond to the case of porous material with large enough surface stresses, when $k^s = 0.5$, and the curves 4 correspond to the case of porous material with very large surface stresses, when $k^s = 1$. Figures 2, 3, 4, 5, 6 and 7 on the left (a) show graphs for the case of a cubic pore, and on the right (b) show similar curves for the case of a spherical pore.

Figures 2, 3, 4, 5, 6 and 7 demonstrate an essential dependence of the effective moduli, both on the pore shape and on the coefficient of surface stresses k^s . These dependencies also differ by module type. So, for moduli characterizing uniaxial tension, shear and transversal deformations, these dependencies are different.

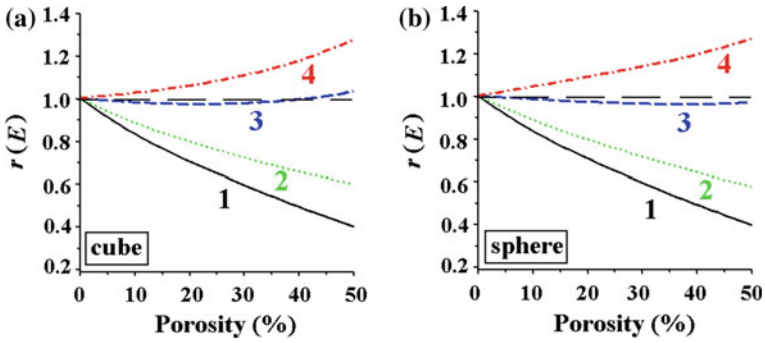


Fig. 2 Dependencies of the relative effective Young's modulus E versus porosity

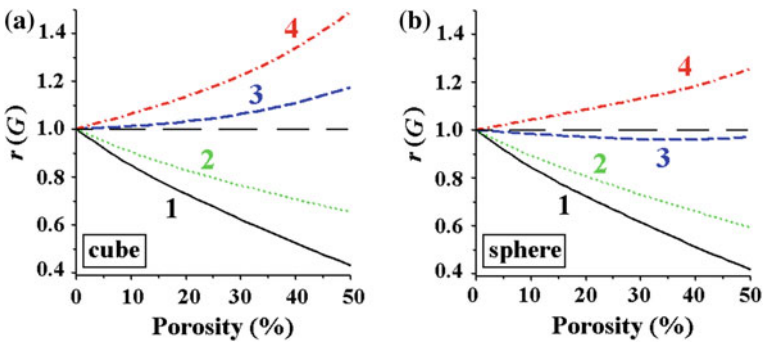


Fig. 3 Dependencies of the relative effective shear modulus G versus porosity

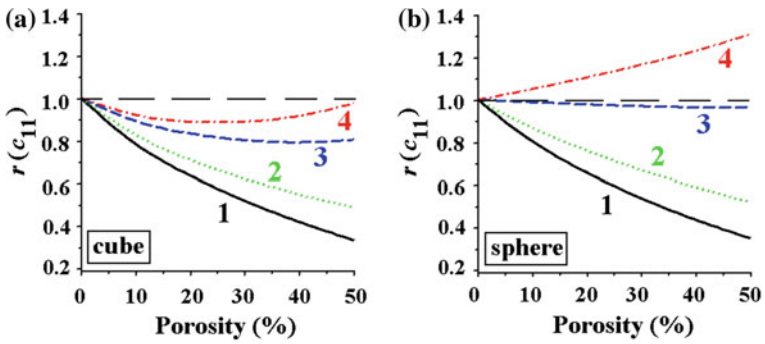


Fig. 4 Dependencies of the relative effective stiffness modulus c_{11} versus porosity

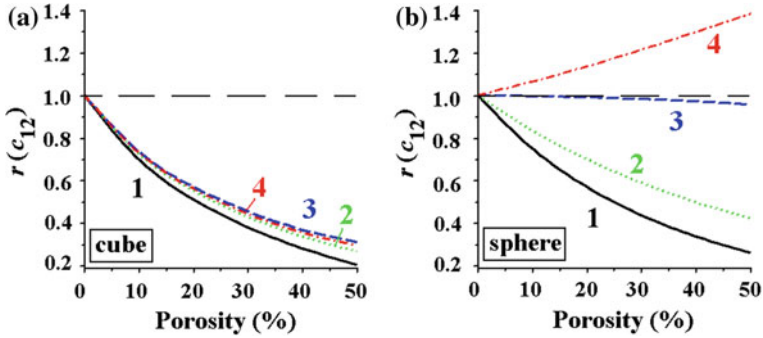


Fig. 5 Dependencies of the relative effective stiffness modulus c_{12} versus porosity

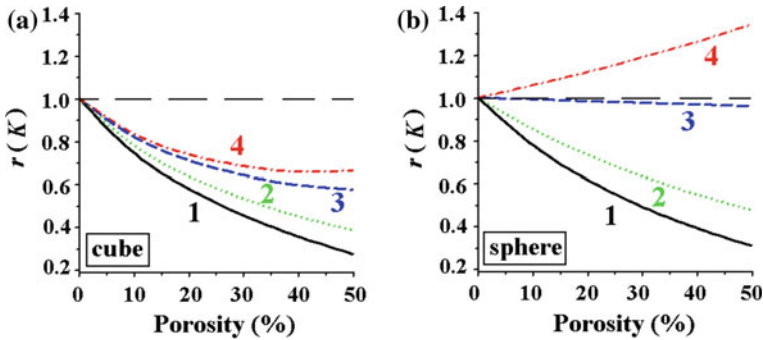


Fig. 6 Dependencies of the relative effective bulk modulus K versus porosity

In the absence of surface stresses (curves 1), all moduli decrease with increasing porosity, and the shapes of the pores have a certain effect, though it is not so extensive. The presence of surface stresses radically changes the pattern of dependencies. All moduli can be subdivided into two groups, in which the dependencies of the moduli on porosity and on the shape of the pores are most similar to each other. The first group includes the moduli characterizing uniaxial tension: the Young’s modulus E , the shear modulus G , and the stiffness modulus c_{11} (Figs. 2, 3 and 4). The second group includes the moduli characterizing transverse deformations and uniform compression: the stiffness modulus c_{12} , the bulk modulus K , and the Poisson’s ratio ν (Figs. 5, 6 and 7).

For very large coefficients k^s for a cubic pore, as the porosity increases, the Young’s modulus E and shear modulus G grow faster than in the case of a spherical pore. On the contrary, the stiffness modulus c_{11} for large k^s grows faster for a spherical pore.

Meanwhile, for the stiffness modulus c_{12} , the bulk modulus K , and the Poisson’s ratio ν , these behaviours differ significantly from porosity. For all used coefficients k^s , these moduli decrease with increasing porosity for a cubic pore. However, for a spherical pore, these moduli increase for large k^s (curves 4). In this case, the most

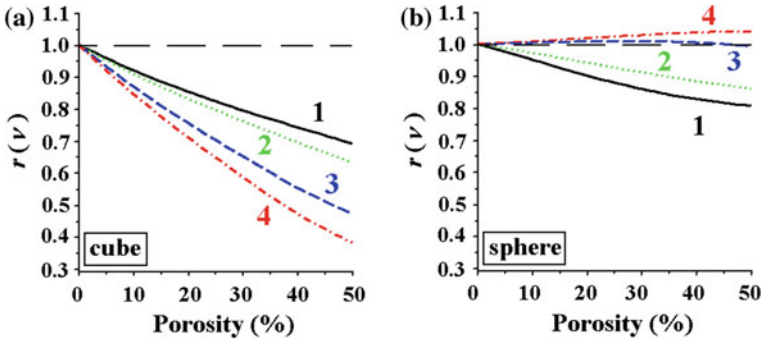


Fig. 7 Dependencies of the relative effective Poisson's ratio ν versus porosity

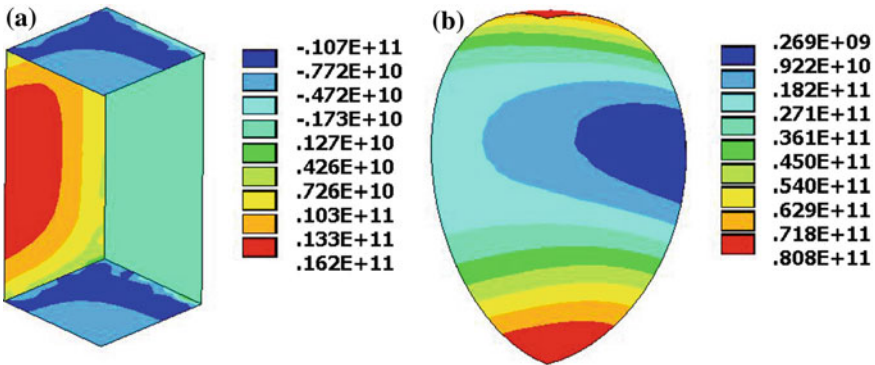


Fig. 8 Stresses σ_{22} in membrane elements for cubic pore (a) and for spherical pore (b)

interesting is the behaviour of the Poisson coefficient ν , which for a cubic pore not only decreases with increasing porosity, but this decrease becomes stronger with increasing k^s , which differs from the corresponding behavior of the stiffness modulus c_{12} and the bulk modulus K .

Such differences can be explained by the fact that for a cubic pore under extension along the x_1 axis, the stresses σ_{22} (and similarly for σ_{33}) in membrane elements change sign, and on edges perpendicular to the axis x_2 do not occur. In the case of a spherical pore, membrane elements are located on curved surfaces. Therefore, with uniaxial tension in membrane elements, the various stress components arise, and the main stresses σ_{11} on a curved surface significantly affect to the stresses σ_{22} and σ_{33} . As can be seen from Fig. 8, the stresses σ_{22} in membrane elements on the sphere surface do not change sign, and their maximum values are almost five times larger than for a cubic pore. Since the stiffness modulus c_{12} according to (11), (12) is calculated by integrating the stresses σ_{22} both by volume elements and surface elements, then it is clear that the surface stresses for a spherical pore increase the modulus c_{12} significantly more than for a cubic pore.

Similar reasoning is true for the bulk modulus K , and it is obvious that the sphere-shaped pore reinforced over the surface gives a more rigid structure for a full compression in the composite than the cubic pore reinforced over the surface.

Thus, summarizing the above, we can conclude that the shape of the pores has a significant influence on the effective moduli of the porous material, especially when taking into account surface stresses for nanoscale pores.

Finally, we can note the well-known fact that for a nanoporous material its effective moduli may be larger than for a solid material. As can be seen in Figs. 2, 3, 4, 5, 6 and 7, these situations occur when the values of the relative effective moduli are greater than 1 (i.e. the curves 3 or 4 turn out to be above the dashed line $r(\dots) = 1$). An explanation of this can be found in many papers [9–11, 26, 27] and therefore is not repeated here.

Further studies can be aimed at solving the problems with periodic boundary conditions, with representative volumes with a large number of pores of different shapes and with the definition of surface moduli by using different formulae that was accepted in this paper.

Acknowledgements This work was supported by the Russian Science Foundation (grant number 15–19–10008-P).

References

1. Brisard, S., Dormieux, L., Kondo, D.: Hashin-Shtrikman bounds on the bulk modulus of a nanocomposite with spherical inclusions and interface effects. *Comp. Mater. Sci.* **48**, 589–596 (2010)
2. Brisard, S., Dormieux, L., Kondo, D.: Hashin-Shtrikman bounds on the shear modulus of a nanocomposite with spherical inclusions and interface effects. *Comp. Mater. Sci.* **50**, 403–410 (2010)
3. Chatzigeorgiou, G., Javili, A., Steinmann, P.: Multiscale modelling for composites with energetic interfaces at the micro- or nanoscale. *Math. Mech. Solids*. **20**, 1130–1145 (2015)
4. Chatzigeorgiou, G., Meraghni, F., Javili, A.: Generalized interfacial energy and size effects in composites. *J. Mech. Phys. Solids*. **106**, 257–282 (2017)
5. Chen, T., Dvorak, G.J., Yu, C.C.: Solids containing spherical nano-inclusions with interface stresses: effective properties and thermal-mechanical connections. *Int. J. Solids Struct.* **44**, 941–955 (2007)
6. Duan, H.L., Wang, J., Huang, Z.P., Karihaloo, B.L.: Eshelby formalism for nano-inhomogeneities. *Proc. R. Soc. A*. **461**, 3335–3353 (2005)
7. Duan, H.L., Wang, J., Huang, Z.P., Karihaloo, B.L.: Size-dependent effective elastic constants of solids containing nano-inhomogeneities with interface stress. *J. Mech. Phys. Solids*. **53**, 1574–1596 (2005)
8. Duan, H.L., Wang, J., Huang, Z.P., Luo, Z.Y.: Stress concentration tensors of inhomogeneities with interface effects. *Mech. Mater.* **37**, 723–736 (2005)
9. Duan, H.L., Wang, J., Karihaloo, B.L., Huang, Z.P.: Nanoporous materials can be made stiffer than non-porous counterparts by surface modification. *Acta Materialia*. **54**, 2983–2990 (2006)
10. Eremeyev, V.A.: On effective properties of materials at the nano- and microscales considering surface effects. *Acta Mech.* **227**, 29–42 (2016)
11. Eremeyev, V., Morozov, N.: The effective stiffness of a nanoporous rod. *Dokl. Physics*. **55**(6), 279–282 (2010)

12. Gad, A.I., Mahmoud. F.F., Alshorbagy. A.E., Ali-Eldin. S.S.: Finite element modeling for elastic nano-indentation problems incorporating surface energy effect. *Int. J. Mech. Sciences.* **84**, 158–170 (2014)
13. Gao, W., Yu, S.W., Huang, G.Y.: Finite element characterization of the size-dependent mechanical behaviour in nanosystem. *Nanotechnology* **17**, 1118–1122 (2006)
14. Gu, S.-T., Liu, J.-T., He, Q.-C.: Size-dependent effective elastic moduli of particulate composites with interfacial displacement and traction discontinuities. *Int. J. Solids Struct.* **51**, 2283–2296 (2014)
15. Gurtin, M.E., Murdoch, A.I.: A continuum theory of elastic material surfaces. *Arch. Rat. Mech. Analysis.* **57**(4), 291–323 (1975)
16. Hamilton, J.C., Wolfer, W.G.: Theories of surface elasticity for nanoscale objects. *Surface Sci.* **603**, 1284–1291 (2009)
17. Javili, A., Chatzigeorgiou, G., McBride, A.T., Steinmann, P., Linder, C.: Computational homogenization of nano-materials accounting for size effects via surface elasticity. *GAMM-Mitteilungen* **38**(2), 285–312 (2015)
18. Javili, A., McBride, A., Mergheima, J., Steinmann, P., Schmidt, U.: Micro-to-macro transitions for continua with surface structure at the microscale. *Int. J. Solids Struct.* **50**, 2561–2572 (2013)
19. Javili, A., McBride, A., Steinmann, P.: Thermomechanics of solids with lower-dimensional energetics: on the importance of surface, interface, and curve structures at the nanoscale. A unifying review. *Appl. Mech. Rev.* **65**, 010802-1–31 (2013)
20. Javili, A., Steinmann, P.: A finite element framework for continua with boundary energies. Part I: the two-dimensional case. *Comput. Methods Appl. Mech. Engrg.* **198**, 2198–2208 (2009)
21. Javili, A., Steinmann, P.: A finite element framework for continua with boundary energies. Part II: The three-dimensional case. *Comput. Methods Appl. Mech. Engrg.* **199**, 755–765 (2010)
22. Jeong, J., Cho, M., Choi, J.: Effective mechanical properties of micro/nano-scale porous materials considering surface effects. *Interact. Multiscale Mech.* **4**(2), 107–122 (2011)
23. Kushch, V.I., Mogilevskaya, S.G., Stolarski, H.K., Crouch, S.L.: Elastic fields and effective moduli of particulate nanocomposites with the Gurtin-Murdoch model of interfaces. *Int. J. Solids Struct.* **50**, 1141–1153 (2013)
24. Le Quang, H., He, Q.-C.: Variational principles and bounds for elastic inhomogeneous materials with coherent imperfect interfaces. *Mech. Mater.* **40**, 865–884 (2008)
25. Miller, R.E., Shenoy, V.B.: Size-dependent elastic properties of nanosized structural elements. *Nanotechnology.* **11**, 139–147 (2000)
26. Nasedkin, A.V., Kornievsky, A.S.: Finite element modeling and computer design of anisotropic elastic porous composites with surface stresses. In: M.A. Sumbatyan (Ed.) *Wave Dynamics and Composite Mechanics for Microstructured Materials and Metamaterials*. Ser. *Advanced Structured Materials*, vol. 59, pp. 107–122. Springer, Singapore (2017)
27. Nasedkin, A.V., Kornievsky, A.S.: Finite element modeling of effective properties of elastic materials with random nanosized porosities. *ycisl. meh. splos. sred* – *Computational Continuum Mechanics.* **10**(4), 375–387 (2017)
28. Nasedkin, A.V., Kornievsky, A.S.: Finite element homogenization of elastic materials with open porosity at different scale levels. *AIP Conf. Proc.* **2046**, 020064 (2018)
29. Nasedkin, A.V., Nasedkina, A.A., Kornievsky, A.S.: Modeling of nanostructured porous thermoelastic composites with surface effects. *AIP Conf. Proc.* **1798**, 020110 (2017)
30. Nasedkin, A.V., Nasedkina, A.A., Kornievsky, A.S.: Finite element modeling of effective properties of nanoporous thermoelastic composites with surface effects. In: Greece. M. Papadarakakis, E. Onate, B.A. Schrefler (eds.) *Coupled Problems 2017 - Proceeding VII International Conference on Coupled Problems in Science and Engineering*, 12–14 June 2017, pp. 1140–1151. Rhodes Island, CIMNE, Barcelona, Spain (2017)
31. Nazarenko, L., Bargmann, S., Stolarski, H.: Energy-equivalent inhomogeneity approach to analysis of effective properties of nanomaterials with stochastic structure. *Int. J. Solids Struct.* **59**, 183–197 (2015)
32. Riaz, U., Ashraf, S.M.: Application of Finite Element Method for the Design of Nanocomposites. In: Musa, S.M. (ed.), *Computational Finite Element Methods in Nanotechnology*, pp. 241–290. CRC Press (2012)

33. Sharma, P., Ganti, S., Bhate, N.: Effect of surfaces on the size-dependent elastic state of nano-inhomogeneities. *Appl. Phys. Lett.* **82**, 535–537 (2003)
34. Tian, L., Rajapakse, R.K.N.D.: Finite element modelling of nanoscale inhomogeneities in an elastic matrix. *Comp. Mater. Sci.* **41**, 44–53 (2007)
35. Wang, J., Huang, Z., Duan, H., Yu, S., Feng, X., Wang, G., Zhang, W., Wang, T.: Surface stress effect in mechanics of nanostructured materials. *Acta Mechanica Solida Sinica.* **24**(1), 52–82 (2011)
36. Wang, K.F., Wang, B.L., Kitamura, T.: A review on the application of modified continuum models in modeling and simulation of nanostructures. *Acta Mech. Sin.* **32**(1), 83–100 (2016)